JET-P(94)58

Progress in Spectroscopic Plasma Diagnostics and Atomic Data

M von Hellermann, P Breger, W G Core, U Gerstel, N C Hawkes, A Howman, R W T König, C F Maggi, A C Maas, A G Meigs, P D Morgan, J Svensson, M F Stamp, H P Summers[1], R C Wolf, K-D Zastrow.

JET Joint Undertaking, Abingdon, Oxfordshire, OX14 3EA, UK.
[1] University of Strathclyde, Glasgow, UK.

Preprint of a Invited paper presented to ICPP 1994, Iguaçu, Brazil, 31 October 1994.

November 1994

ABSTRACT

The paper illustrates the role of quantitative spectroscopy for the diagnosis of fusion plasmas and the importance of extensive consistency checks. Four examples are given of recent spectroscopic observations which have triggered new approaches both to plasma modelling and atomic excitation processes. The examples highlight the role of passive charge exchange emission and its implication for plasma edge physics, non-thermal features in the HeII spectrum and temperature anisotropies observed in high power neutral beam heated plasmas, the importance of geometric mapping in an arbitrary magnetic configuration for the evaluation of line integrated spectra, and finally the complexity of atomic processes involved in the spectral analysis for helium transport studies.

INTRODUCTION

Quantitative spectroscopy plays a significant role in the deduction of plasma parameters within the overall framework of diagnosing a hot fusion plasma. The measurement of accurate ion temperatures, well resolved in space and time and the use of absolutely calibrated measurements of spectral line intensities in the subsequent deduction of local ion densities have contributed significantly to a renaissance of plasma spectroscopy and its recognition as an essential diagnostic tool, cf. [1]. The practical implementation of quantitative spectroscopy can best be described as a cycle of modelling, predictions, observations, consistency checks with further refinement at each cycle (Fig.1) cf. [2,3]. The atomic modelling of excitation processes, and its proper adaptation to the plasma environment by inclusion of collisional radiative processes, enables the prediction of local and global (line-of-sight-integrated) spectral features, [4,5]. The successful deduction of plasma parameters is based on a parametric description of spectral features in terms of local plasma data (temperature, density, magnetic field strength etc.) and then the comparison of these spectral predictions with experimental observations.

High core ion temperatures (>20 keV) of present fusion devices imply that the confined plasma region (see Fig.2) contains only fully stripped ions, that is ions not radiating any line emission, with the exception of a very small fraction ($<10^{-4}$) of helium- or hydrogen-like high-Z impurities (Ni, Fe etc.). Then in a narrow region close to the last closed flux surface (LCFS), or magnetic separatrix, there is evidence for line emission following passive charge exchange processes with a dense neutral particle population created by plasma ions reflected and neutralised at the plasma wall. Finally, near the vessel walls, the third type of emission process occurs, that is impact excitation of low-temperature (<0.5keV) partially ionised impurities.

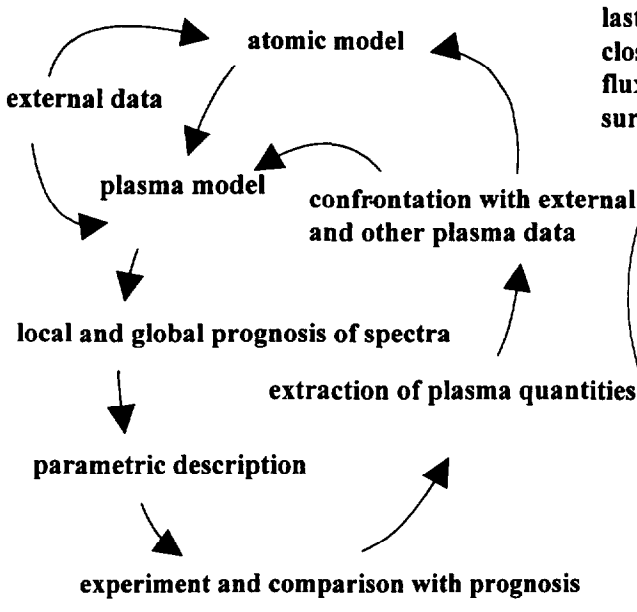

Fig.1 The diagnostic loop as basis of quantitative spectroscopy

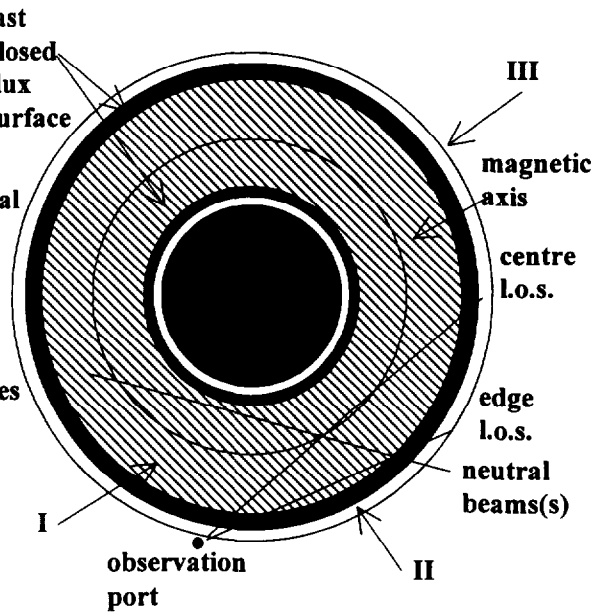

Fig.2 Schematic representation of emission layers and lines of sight in a hot fusion plasma I) plasma core with fully stripped ions (T>5 keV), line radiation following CX interaction with neutral beams, II) intermediate layer close to magnetic, separatrix, T<5keV, line radiation dominantly excited by CX interactions with neutrals, III) plasma wall, partially stripped ions, line radiation by impact excitation, T<1 keV

PASSIVE CHARGE EXCHANGE FEATURES CLOSE TO THE SEPARATRIX

Low energy passive charge exchange excitation processes involving light species play an important role for the emission layers close to the outermost magnetic flux surface of a confined plasma. The present understanding of this process is that deuterium or hydrogen atoms are created as plasma ions hit the wall and then are reflected as neutrals with two or three times the thermal energy, they then interact with fully stripped light impurity ions close to the separatrix. A simple, schematic, model (Fig.3) illustrates impurity ion density profiles, the decay length of the neutral density and also the role of thermal energy in the effective charge capture coefficient. In a recent paper effective emission rates for UV and visible transitions were modelled for capture from hydrogen in its ground and excited-state, cf. [6].

An puzzling observation, which is made in most high-power JET H-mode plasmas, is a flat ion temperature profile (or even a positive ion temperature step) across the magnetic boundary, i.e. an apparent increase of ion temperature beyond the confined plasma region. Similar observations (using a poloidal viewing fan) indicating a flat ion temperature profile

beyond the separatrix were reported recently [7]. In the JET case the apparent ion temperature increase cannot be explained by a toroidal velocity shear across the CX volume. The most likely reason is that for the outermost CX l.o.s (Fig.2), which intersects the neutral beam close to the separatrix, in a region where the C^{6+} density drops rapidly, the passive CX emission overweighs the intensity of the active CX emission. The passive CX emission rate Q(T) depends on the local thermal velocity, the C^{6+} ion density and on the neutral density (Fig.3). Passive charge exchange emission features can be observed from most ionisation stages of impurity ion spectra emitted close to the plasma boundary, for example, the CIII(n=7→n=5) and CVI(n=8→n=7) spectra (Fig.4). The differential effect between electron impact excitation and charge transfer in forming the highly excited emitting ion population suggests that the influence of the hydrogen donor population can be distinguished and thus a neutral hydrogen density close to the separatrix may be deduced.

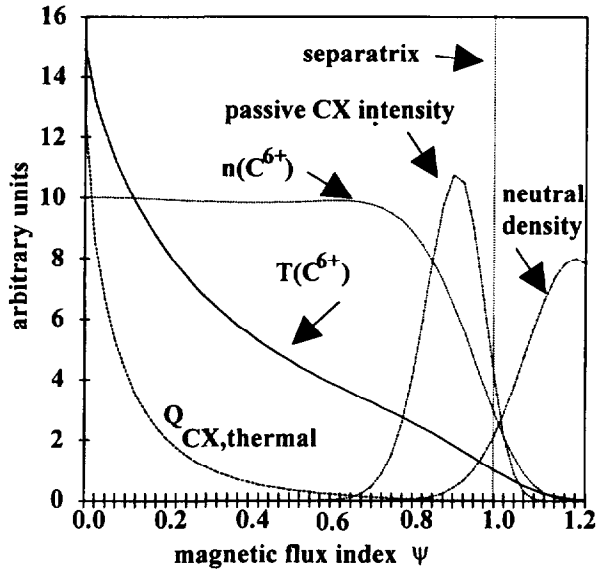

Fig.3 Schematic model for thermal CX excitation, based on a neutral density layer, a CVI density profile, and an emission rate Q which depends on the local thermal energy

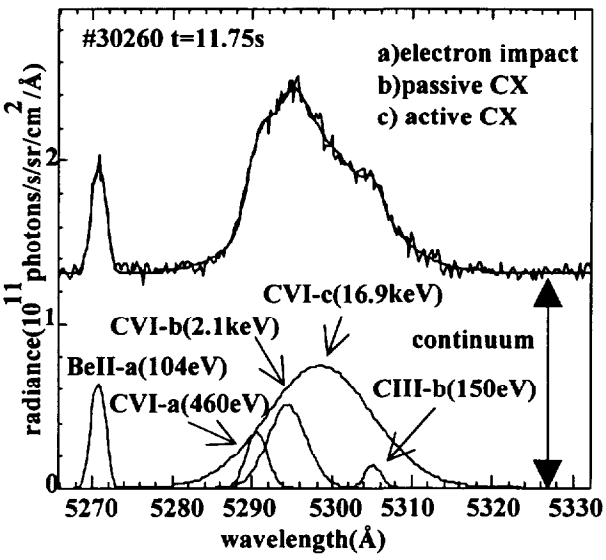

Fig.4 The CVI spectrum illustrating a) impact excitation, b) passive and c) active charge exchange.

HIGH POWER NEUTRAL BEAM HEATING AND TEMPERATURE ANISOTROPY

Many of the present fusion experiments are characterised by substantial 'auxiliary' heating. In fact the 'added' heating power may exceed the 'ohmic' heating power by more than an order of magnitude. Recent milestones of fusion yield and ion temperatures, for example, have been achieved with neutral beam powers of 20 to 30 MW. At this power level a significant proportion of the plasma ion velocity distribution function is affected within the period of the slowing-down time of the injected fast particles. A distinctive distortion of the bulk plasma

velocity distribution function occurs, cf. [8]. As a result of this, apparent ion temperatures measured spectroscopically perpendicular and parallel to the magnetic field may differ considerably. This phenomenon was reported for the first time in low-target-density high-power helium-neutral-beam-heating-plasmas, cf. [9], where strongly anisotropic alpha particle thermal distribution functions were observed. That is, strong differences in temperatures deduced from essentially Maxwellian HeII spectra are observed in directions parallel and perpendicular to the magnetic field. The term 'temperature' in this context is inappropriate and should be replaced by the second moment of a generalised (not necessarily Maxwellian) anisotropic velocity distribution function:

$$T_{perp} = \frac{1}{2} M \langle v^2 \rangle_{perp} = \frac{1}{2} M \int d^3v \cdot v^2 \cdot f_{perp}(\vec{v})$$

and

$$T_{par} = \frac{1}{2} M \langle v^2 \rangle_{par} = \frac{1}{2} M \int d^3v \cdot v^2 \cdot f_{par}(\vec{v})$$

The degree of anisotropy (i.e. $T_{perpendicular}:T_{parallel}$) increases with the local source rate of non-thermal particles. It is a sensitive function of the injection pitch angle (for the JET injection geometry the pitch angle is approximately 62°). The anisotropy reaches a peak value within a slowing-down-time and vanishes again in a period corresponding to one or two slowing-down times. During the decay of the anisotropy the thermal population builds up

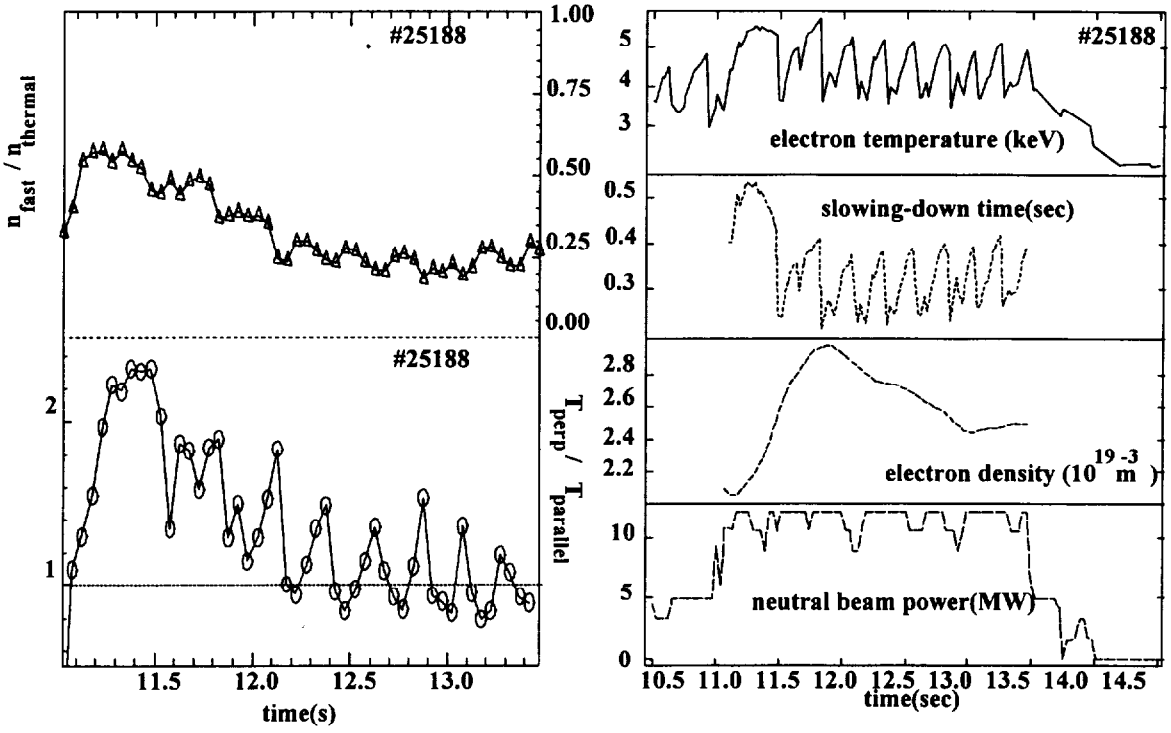

Fig.5 Temperature anisotropy observed in high power neutral helium beam heating experiment

continuously (the thermal particle confinement time is 1 to 3 sec) and the fast alpha particle concentration is reduced to a small fraction. Since the source rate profile is strongly peaked it is expected that a noticeable anisotropy can only persist close to the magnetic axis. Sawtooth activity also strongly affects the anisotropy indicating that it is an efficient mixing mechanism removing fast particles from the plasma core. At the collapse of each sawtooth, approximately isotropic conditions are re-established, and subsequently the anisotropy builds up again to a level determined by the slow decay following the peak at about 0.5s after the high power beams were switched on (cf. Fig.5).

A conclusion which can be drawn from this observation and also from theoretical modelling of the anisotropic neutral injection Fokker-Planck equation, cf. [8], is that, for present fusion devices, where high levels of neutral beam power injected into comparatively small plasma volumes lead to a substantial fraction of non-thermal fast particles, the observed temperatures do not necessarily represent a steady state population nor an isotropic Maxwellian distribution function.

HELIUM TRANSPORT EXPERIMENTS

The close link between atomic data provision for spectroscopic analysis and progress in the deduction of usable plasma data is particularly striking in the case of charge exchange spectroscopy of HeII. Over the last few years new experimental data and theoretical calculations have provided an extensive database on atomic processes relevant for the interaction of neutral

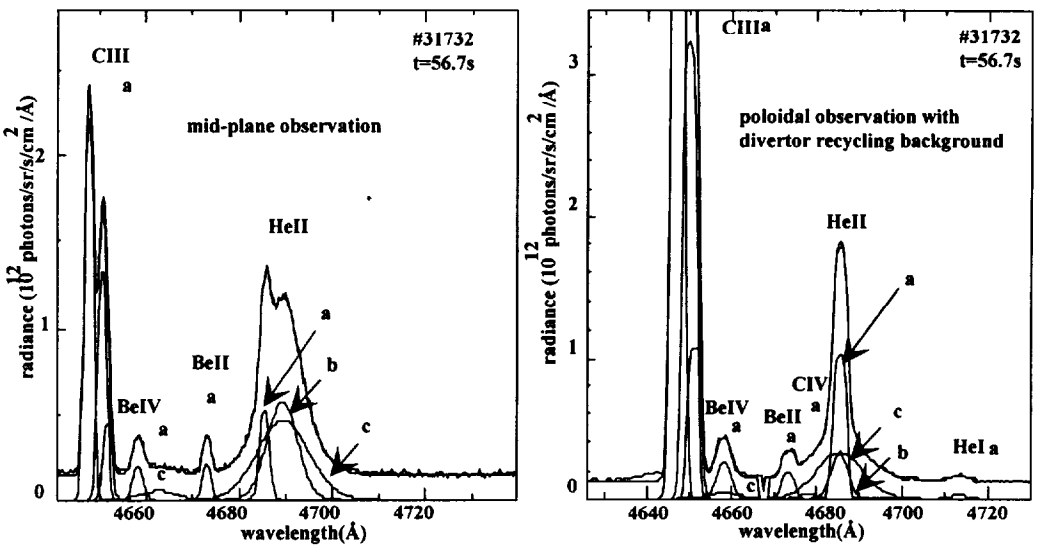

Fig.6 The HeII, CIII, BeII and BeIV spectrum with three excitation components a) electron impact, b) passive charge exchange c) active charge exchange. Left: Torus mid-plane observation. Right: Vertical line of sight viewing parts of the JET divertor target plates. In the case of enhanced recycling weak CIV lines are observed at 4677Å(6d8f) and 4735Å(6d8p).

beams and plasma ions and electrons. The database, cf. [10,11,12] includes neutral beam attenuation cross-sections, excitation rates by neutral hydrogen or helium beams acting as a donor, collisional excitation of fast beam particles (beam emission spectroscopy, cf. [13]), the prediction of enhancement factors due to donor populations in excited or metastable states and also data required for the modelling of the neutral beam associated plumes, cf. [14]. The assessment of plume contributions requires detailed calculations including magnetic configurations, geometrical factors, and ionisation and excitation rates for He^+ ions travelling along field lines into the CX observation line. In addition, the contributions of passive charge exchange to the HeII spectrum, the so-called 'luke-warm' component, represents a further complication in the analysis.

It is tempting to eliminate the problems related to the complexity of passive edge emission spectra by applying subtraction- or beam modulation-techniques. In the first case spectra gained by an independent viewing system, which does not collect any active spectra, are subtracted. In the second case, spectra measured subsequently during beam-on and beam-off periods are subtracted. However, in both cases it is essential to provide confirmatory independent measurements of, for example, ion temperatures derived from X-ray spectroscopy or other CX spectra to ensure data consistency.

Experimental transport studies rely on controlled perturbations of impurity density profiles. For example, edge fuelling, cf. [15,16], or core fuelling using neutral helium beam injection, cf. [9]. In each case the transient changes of local density gradients and radial particle fluxes provide in the source-free plasma region the means for the deduction of diffusion coefficients D and convective velocity v. In order to derive gradients in time and space usually analytical profile functions are introduced and smoothed time traces are needed. Fig.7 shows an example of helium edge fuelling, where a 100ms puff was added during a JET H-mode phase. Radial profiles $n_z(\rho) = n_z(0)\cdot(1-\rho^2)\cdot(1+p\cdot\rho^2+q\cdot\rho^4)$, where is the normalised minor radius, are fitted to the experimental data. The selected time window for the evaluation of particle flows $\Gamma_z(\rho) = \frac{dr/d\rho}{dV/d\rho}\cdot\frac{d}{dt}\int_0^\rho dV\cdot n_z(\rho)$ and gradients ∇n_z and the subsequent analysis of $\frac{\Gamma_z}{n_z} = -D\frac{\nabla n_z}{n_z} + v_z$ may be a critical issue. Error propagation of experimental data will possibly lead to substantial uncertainties in deduced transport coefficients.

An alternative approach to the evaluation of transport experiments is the adaptation of prediction codes to experimentally observed profiles and the deduction of transport coefficients (cf. [17]).

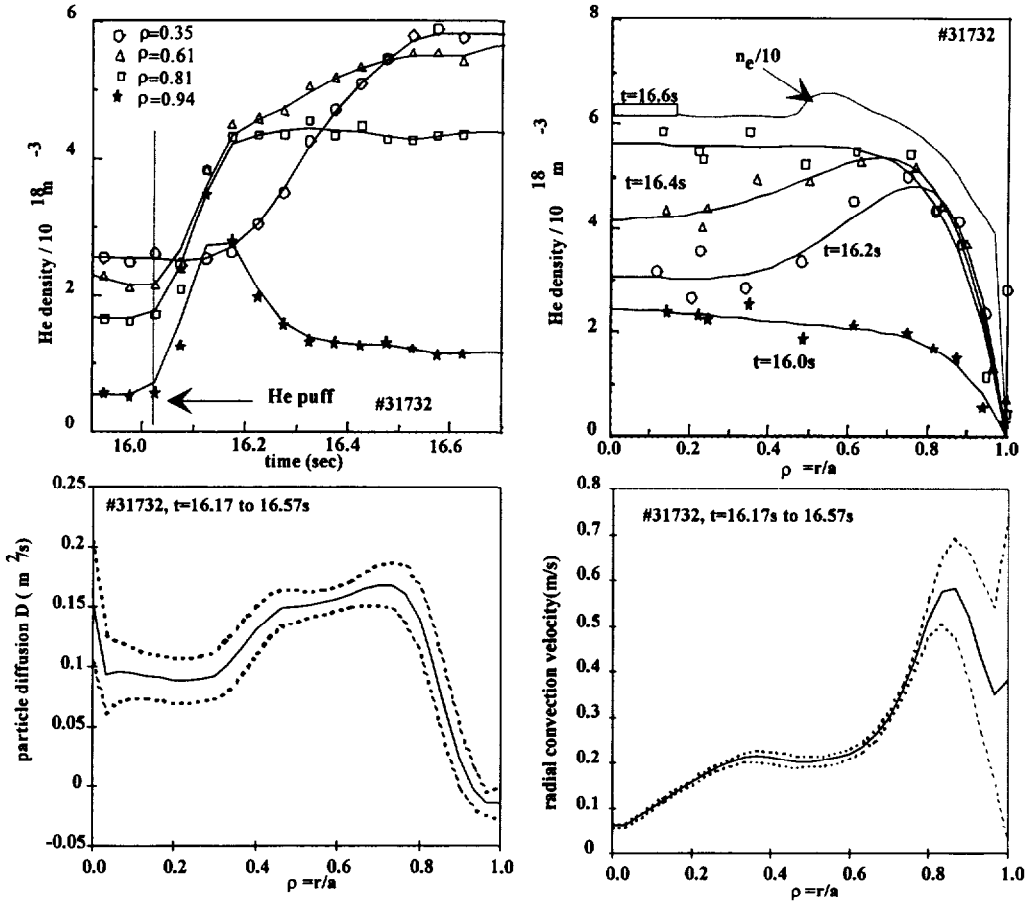

Fig.7 Helium transport studies based on plasma edge gas puffing during a H-mode phase, a) time history at 4 different radii, b) radial profiles following the gas puff, and for comparison, a scaled-down electron density profile (n_e/10). Central (H-mode) helium densities reach a steady state level in 0.5s. Particle diffusion coefficients c) and convection velocities b) are derived from $\Gamma(\rho)/n_z(\rho)=-D(\rho)\nabla n_z(\rho)/n_z(\rho)+v(\rho)$ for the 0.4s time interval, 16.17s to 16.57s, in which the helium density profile relaxes to an electron-density-like profile.

MERGING OF ACTIVE AND PASSIVE DIAGNOSTIC TECHNIQUES

Local measurements are of course not the only route by which quantitative deductions can be made from spectroscopic results, although clearly preferred. The following two examples illustrate how a combination of localised data, especially electron density and electron temperature provided by Thomson scattering, atomic modelling of local emissivities and non-localised, line of sight integrated spectroscopic measurements yield useful quantitative results. The first example is the measurement of continuum radiation in the visible wavelength range and the deduction of a line averaged $<Z_{eff}>$. The second example is the deduction of a semi-localised ion temperature value from the X-ray spectrum of helium-like nickel. In both cases the mapping of the line of sight and that of electron temperature and density profiles onto a common magnetic flux surface geometry is crucial. In the first example, for each point along the line of sight, the values for electron density and temperature $n_e(\rho=r/a)$, $T_e(\rho)$ and that of the free-free

Gaunt factor $g_{ff}(T(\rho), \lambda)$ need to be calculated. Assuming that each flux surface represents a constant value of Z_{eff} then any line-of-sight-integrated measurement of continuum radiation is characterised by its impact radius $_{min}$, that is its smallest minor flux radius, see Fig.8. This approach enables the reconstruction of an Abel inverted $Z_{eff}(\rho)$ profile, and moreover, provides the means for cross-calibrations for any line of sight crossing the plasma in arbitrary geometry. The latter aspect is of great importance for most of the spectroscopic collection optics whose window transmissions may deteriorate substantially during extensive operation periods, and the access to a common radiation source, which is toroidally and poloidally symmetric, has proven to be a powerful asset for consistency checks.

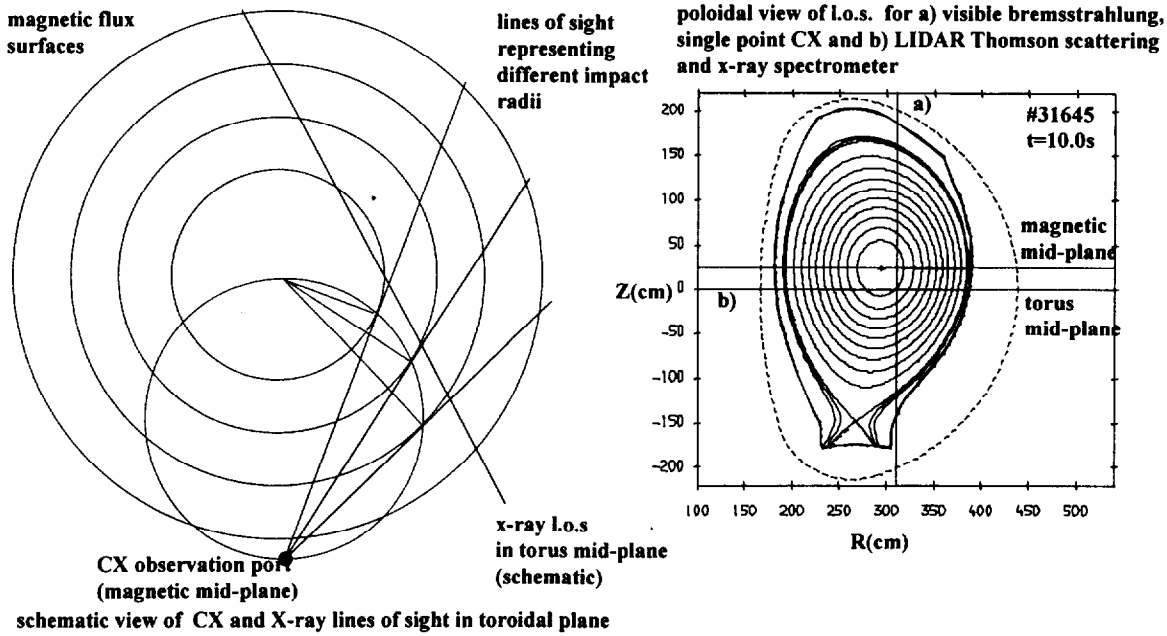

Fig.8 Schematic display of JET l.o.s. in toroidal and poloidal plane. Left: Mid-plane fan for CX and continuum, top view of x-ray l.o.s. Right: lines of sight in poloidal plane for a) CX and continuum, b) LIDAR and X-ray

A similar procedure is applied in the second example, the JET high resolution X-ray spectrometer. In this case a single line of sight, and its corresponding vector of intersected flux surfaces, is used to derive an emission expectation value <(t)> for the location and width of the emission shell.

$$<\rho>=\frac{\int \rho \cdot w(\rho) d\rho}{\int w(\rho) d\rho} \quad \text{with:} \quad w(\rho) = f_{NiXXVII}(T_e(\rho)) \cdot n_e^2(\rho) \cdot \varepsilon(T_e(\rho)) \cdot g(\rho)$$

where f is the local fraction of helium-like nickel, the emissivity, and g a geometry factor. The width of the emission layer ($\sigma_\rho = \sqrt{<\rho^2> - <\rho>^2}$) is calculated by the second moment of the weighting function. The JET x-ray spectrometer line-of-sight passes below the magnetic mid-plane and the effective emission shell position varies in the range $0.15<<0.35$ subject to

changes of electron density and temperature profiles. Note, that the emissivity of NiXVVII reaches its maximum at 8 keV and the peak intensity is not necessarily on-axis [5].

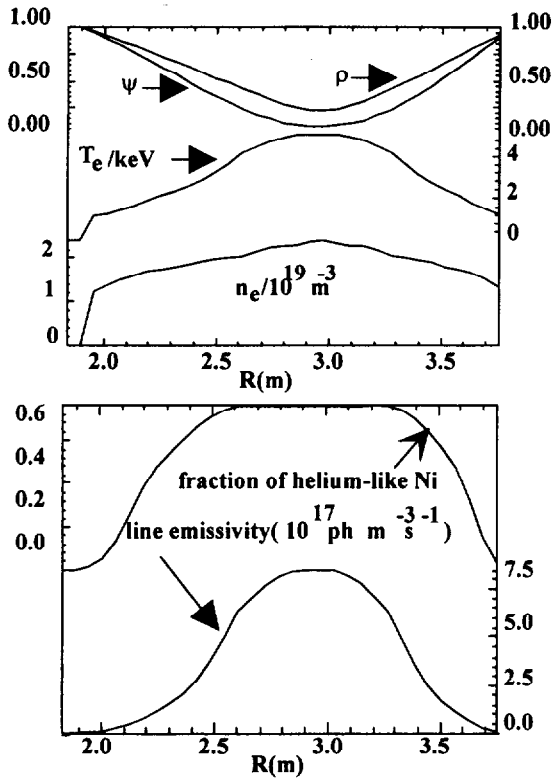

Fig.9 Top: flux index, minor radius, T_e, n_e. Bottom: line emissivities versus radius.

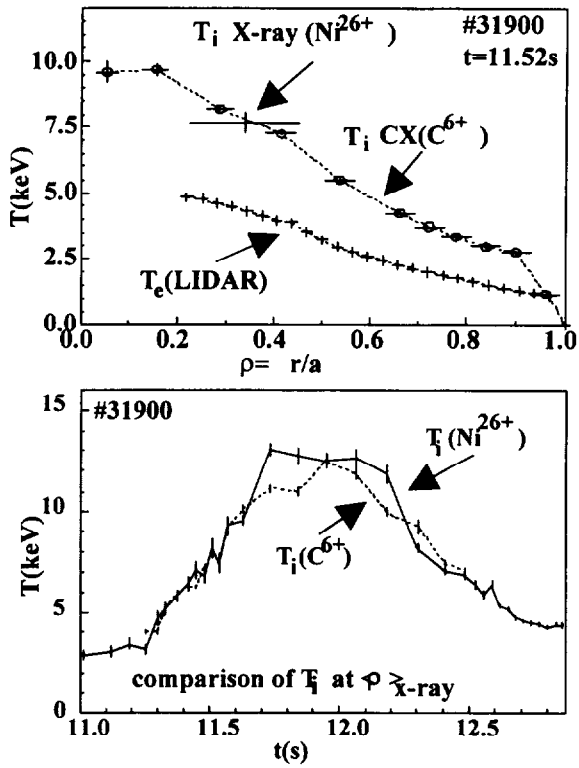

Fig.10 Combined active and passive diagnostic techniques. The time trace shows T_i(x-ray) and T_i(CVI) at <(t)>

SUMMARY

Substantial progress has been achieved over the last decade in the expansion of atomic data bases for fusion plasmas and in derived data used in experimental analysis. The deduction of absolute particle densities within the magnetically confined plasma based on charge exchange spectroscopy has become an advanced technique in use in many fusion laboratories. However, the need for consistency checks involving the entire plasma environment has become increasingly necessary and wide spread in their scope. This is very demanding in terms of data range, quality and integration. In particular, the plasma edge and divertor region is still difficult to assess, so that local or semi-local spectroscopic measurements leading to absolute particle densities rather than incompletely analysed photon counts, are a major challenge. In the confined plasma region, the diagnosis of high energy alpha particles will need considerable future efforts. A combination of active and passive spectroscopic techniques is possibly the most promising way for future fusion devices with reduced access and enhanced radiation levels.

ACKNOWLEDGEMENT

The authors are much indebted to the stimulating impact of D. Hillis and M. Wade (ORNL) on helium transport experiments.

REFERENCES

[1] R.Isler, Plasma Physics and Contr. Fusion, **36**, 171(1994)

[2] M von Hellermann and H.P. Summers, Rev.Sci.Instr. **63**, 5132(1992)

[3] M. von Hellermann and H.P.Summers, Atomic and Plasma Material Interaction Processes in Controlled Thermonuclear Fusion, Ed. Janev, 'Elsevier Science Publishers 1993',135-164

[4] H.P.Summers and M. von Hellermann, Atomic and Plasma Material Interaction Processes in Controlled Thermonuclear Fusion, Ed. Janev, 'Elsevier Science Publishers 1993',87-117

[5] K.-D. Zastrow, H.W.Morsi, M. Danielsson, M.G. von Hellermann, E. Källne, R. König, W.Mandl, H.P.Summers, J. Appl. Phys, **70**, 6732 (1991)

[6] C.F. Maggi, L.D.Horton, R.König, M.Stamp, 21st EPS Conf. Contr. Fus. & Plasma Physics, Montpellier 1994

[7] W.Mandl, K.H.Burrell, R.J.Groebner, J.Kim, R.P.Seraydarian, M.R.Wade, J.T.Scoville, To Appear in Nuclear Fusion 1994

[8] W.G.F.Core, to be published

[9] M von Hellermann, W.G.F.Core, J.Frieling, L.D.Horton, R.W.T. König, W.Mandl, H.P.Summers, Plasma Phys. Contr. Fusion,**35**,799, 1993

[10] H.P.Summers, 'The JET Atomic Data and Analysis Structure', JET-IR(1994)

[11] H.P.Summers, Adv. At. Mol. Opt. Physics, **33**, 275(1994)

[12] H.O. Folkerts, R. Hoekstra, L.Meng, R.E. Olson, W.Fritsch, R. Morgenstern, H.P.Summers, J.Phys.B:At.Mol.Opt.Phys.**26**(1993)619

[13] W.Mandl, R.Wolf, M von Hellermann, Plasma Phys. Contr. Fusion,**35**,1373, 1993

[14] R.Fonck, D.S Darrow, K.P. Jaehnig et al., Phys.Rev. (1984) **29**,3288

[15] M.R.Wade, D.L.Hillis, J.T.Hogan, M.A.Mahdavi, R.Maingi, W.P.West, N.H.Brooks, K.H.Burrell, R.J.Groebner, G.L.Jackson, C.C.Klepper, G.L.Laughon, M.M.Menon, P.K.Mioduszewski and DIII-Team Submitted to Phys.Rev.Let., 1994, GA-A21652

[16] D.L.Hillis, M.R.Wade, J.T.Hogan, M.A.Mahdavi, R.Maingi, W.P.West, N.H.Brooks, K.H.Burrell, D.F.Finkenthal, R.J.Groebner, G.L.Jackson, C.C.Klepper, G.L.Laughon, M.M.Menon, P.K.Mioduszewski, 15th International Conf. Plasma Physics, Seville, Spain, October 1994

[17] L.Lauro-Taroni, B.Alper, R.Giannella, K.Lawson, F.Marcus, M.Mattioli, P.Smeulders, M.von Hellermann, 21st EPS Conf. Contr. Fus. & Plasma Physics, Montpellier 1994